

# Neutrino Oscillations Experiments using Off-axis NuMI Beam

*February 7, 2008*

A. Para, Fermilab

M. Szleper, Northwestern University

## Abstract

NuMI neutrino beam is constructed to aim at the MINOS detector in Soudan mine. Neutrinos emitted at angles  $10 - 20$  *mrad* with respect to the beam axis create an intense beam with a well defined energy, dependent on the angle. Additional surface detectors positioned at the transverse distance of several kilometers from the mine offer an opportunity for very precise measurements of the neutrino oscillation parameters. The mixing matrix element  $|U_{e3}|^2$  can be measured down to a value of 0.0025 with the exposure of the order of  $20$  *kton*  $\times$  *years*.

# Contents

<b>1</b>	<b>Introduction</b>	<b>3</b>
<b>2</b>	<b>The NuMI Beams</b>	<b>3</b>
<b>3</b>	<b>The Principle of Off-axis Neutrino Beams</b>	<b>4</b>
<b>4</b>	<b>Off-axis Beams at NuMI</b>	<b>7</b>
4.1	Low Energy Beam Case . . . . .	7
4.2	Medium Energy Beam Case . . . . .	7
4.3	High Energy Beam Case . . . . .	8
<b>5</b>	<b><math>\nu_\mu</math> Disappearance Experiment with the Off-axis Detectors</b>	<b>8</b>
<b>6</b>	<b>Systematics I: Understanding of the Beam Spectra</b>	<b>11</b>
<b>7</b>	<b>Systematics II: Backgrounds</b>	<b>12</b>
<b>8</b>	<b><math>\nu_e</math> Appearance Experiment</b>	<b>13</b>
<b>9</b>	<b>Neutrino Detectors Issues</b>	<b>19</b>
<b>10</b>	<b>Acknowledgments</b>	<b>21</b>

## List of Figures

1	High, medium and low energy options for NuMI beams. Histograms represent the rates of $\nu_\mu$ CC events expected at the distance of 730 km in a detector with 1 kton fiducial volume. . . . .	4
2	Variation the neutrino energy with the decay angle $\theta_{dec}$ for neutrinos produced by $\pi$ 's of different energies. . . . .	5
3	Variation the neutrino flux with the decay angle $\theta_{dec}$ for neutrinos produced by $\pi$ 's of different energies. . . . .	6
4	Low energy beam option: neutrino event spectra for 10 kton*years exposure at the detectors on-axis and at 5,10 and 20 km distance. . .	8
5	Contribution of pion- and kaon-produced neutrinos to the neutrino flux at the detectors on-axis and at 5,10 and 20 km distance, low energy beam. . . . .	9
6	Medium energy beam option: neutrino event spectra for 10 kton*years exposure at the detectors on-axis and at 5,10 and 20 km distance. . .	10
7	High energy beam option: neutrino event spectra for 10 kton*years exposure at the detectors on-axis and at 5,10 and 20 km distance. . .	11
8	Expected $\nu_\mu$ CC event rates it the on- and off-axis detectors for 10 kton*years exposure in the medium energy beam. The histogram represents 'no-oscillation' case. The cross-hatched distribution shows the expected rate in case of oscillations with full mixing and $\Delta m^2 = 3.0 \times 10^{-3} eV^2$ . . . . .	12
9	Dependence of the predicted neutrino spectrum on the hadron production model for the case of the low energy beam. Four overlaid histograms represent the expected spectra at different detector positions derived from the spectrum observed at the near detector using different hadron production models. . . . .	13
10	Dependence of the predicted neutrino spectrum on the hadron production model for the case of the medium energy beam. Four overlaid histograms represent the expected spectra at different detector positions derived from the spectrum observed at the near detector using different hadron production models. . . . .	14
11	$\nu_\mu$ and $\nu_e$ induced CC event rates at the on- and off-axis detectors, low energy beam. The upper histogram represents the $\nu_\mu$ rates, the lower one shows the $\nu_e$ rates. . . . .	15
12	$\nu_\mu$ and $\nu_e$ induced CC event rates at the on- and off-axis detectors, medium energy beam. The upper histogram represents the $\nu_\mu$ rates, the lower one shows the $\nu_e$ rates. . . . .	16
13	Sensitivity of the appearance experiments to $ U_{e3} _{min}^2$ for low energy beam exposure 20 kt*years. . . . .	17
14	Sensitivity of the appearance experiments to $ U_{e3} _{min}^2$ for medium energy beam exposure of 20 kt*years. . . . .	18

15	Rates of $\nu_\mu$ CC event rates in the detectors located at different locations. Rates correspond to the medium energy beam, $10\text{ kton} \times \text{year}$ exposure . . . . .	20
----	---	----

## 1 Introduction

A discovery of the neutrino oscillations by the SuperK[1] experiment has changed the neutrino physics. The existence of the phenomenon is no longer in question and the focus of the experiments has changed from the 'discovery' to the 'elucidation'. The next round of experiments, running or under construction, will provide an independent verification of the SuperK result and it is likely confirm that  $\nu_\mu$  neutrinos oscillate mostly into  $\nu_\tau$  with neutrinos with a characteristic frequency corresponding to  $\Delta m^2 \sim 1.5 - 4 \times 10^{-3} \text{ eV}^2$ .

Questions related to neutrino masses and oscillations are of a fundamental nature therefore a significant effort is dedicated to a possible design of the future facilities: high intensity conventional neutrino beams, often referred to as 'superbeams', and/or a novel facility, 'neutrino factory', where a very intense mixed beam of  $\nu_\mu$ 's and  $\nu_e$ 's is produced from decay of muons circulating in a storage ring.

In this note we examine a potential extension of the utilization of the NuMI beam, being constructed at Fermilab, by addition of new detectors. These new detectors could offer a major enhancement of the physics reach of the MINOS detector, especially in conjunction with the anticipated improvements of the Fermilab's accelerator complex.

## 2 The NuMI Beams

Neutrino beam constructed at Fermilab has a flexible design[2]. Focusing elements, consisting of two parabolic horns, can be moved with respect to the target and to each other thus focusing different momentum bytes of the produced pions and giving rise to the neutrino beams of different energies.

The resulting beams are presented in Fig.1 showing the event spectra for a nominal  $1\text{ kton} \times \text{year}$  exposure at the distance of 730 km from the target. In this paper we assume the proton flux on target to be  $3.8 \times 10^{20}$  per year.

The horn acceptance is defined in terms of the relative momentum spread  $\frac{\Delta p}{p}$  producing the neutrino beam with the energy spread increasing with the beam energy. The long tail of the high energy neutrinos in the low and medium energy beams is due to the bare target component of the beam created by high momentum pions traversing the opening in the magnetic horns.

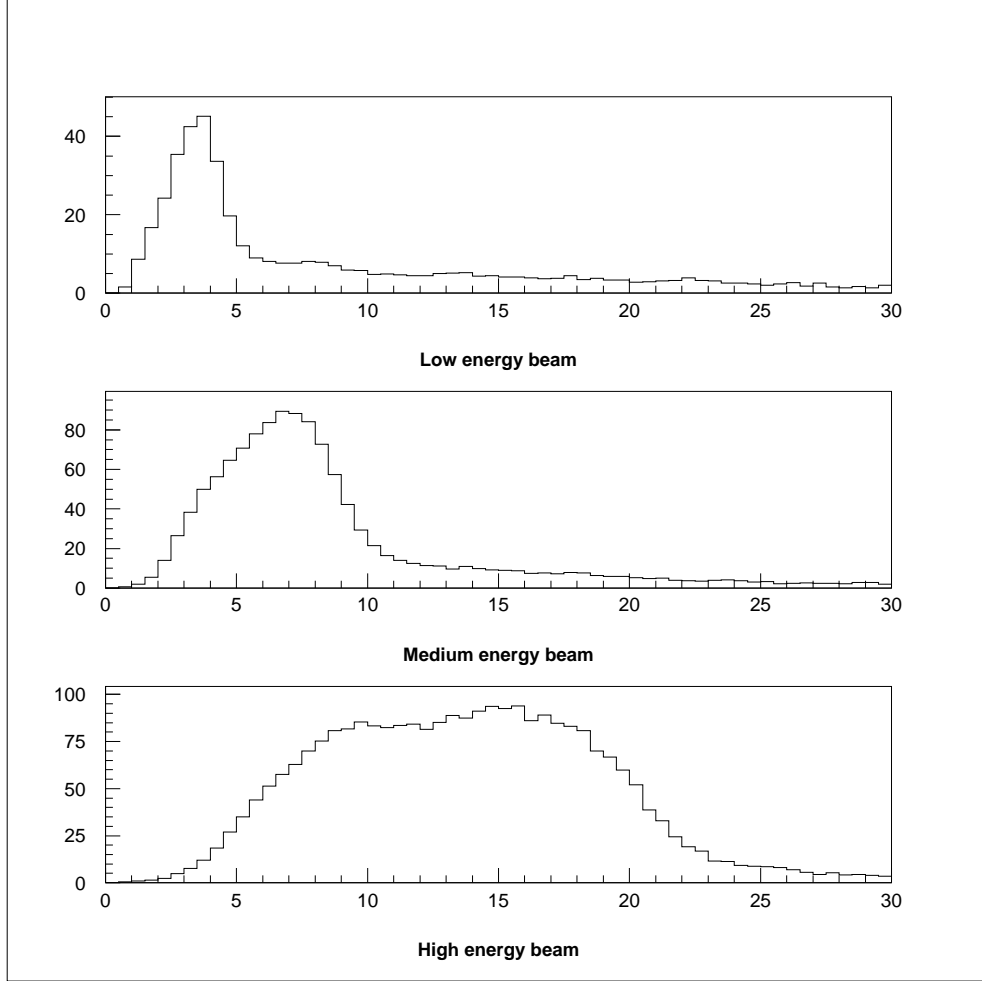


Figure 1: High, medium and low energy options for NuMI beams. Histograms represent the rates of  $\nu_\mu$  CC events expected at the distance of  $730\text{ km}$  in a detector with  $1\text{ kton}$  fiducial volume.

### 3 The Principle of Off-axis Neutrino Beams

Most of the neutrinos in a conventional neutrino beam are produced in two-body decays  $\pi^+ \rightarrow \mu^+ + \nu_\mu$ . A smaller contribution to the beam is due to  $K_{\mu 3}$  decays,  $K^+ \rightarrow \mu^+ + \nu_\mu$ , and to the decays of the muons,  $\mu^+ \rightarrow e^+ \bar{\nu}_\mu \nu_e$ .

Energy and the flux of the neutrinos produced in two-body decays is uniquely determined by the decay angle  $\theta_{dec}$ . For small angles they can be expressed as:

$$E_\nu = \frac{0.43 E_\pi}{1 + \gamma^2 \theta_{dec}^2} \quad (1)$$

$$Flux = \left( \frac{2\gamma}{1 + \gamma^2 \theta_{dec}^2} \right)^2 \frac{A}{4\pi z^2} \quad (2)$$

where

- $\gamma = \frac{E_\pi}{m_\pi}$  is the Lorentz boost factor of a pion
- $\theta_{dec}$  is decay angle, i.e. the angle between the pion and the produced neutrino directions
- $A$  is the area of the detector and  $z$  is the distance between the decay point and the detector.

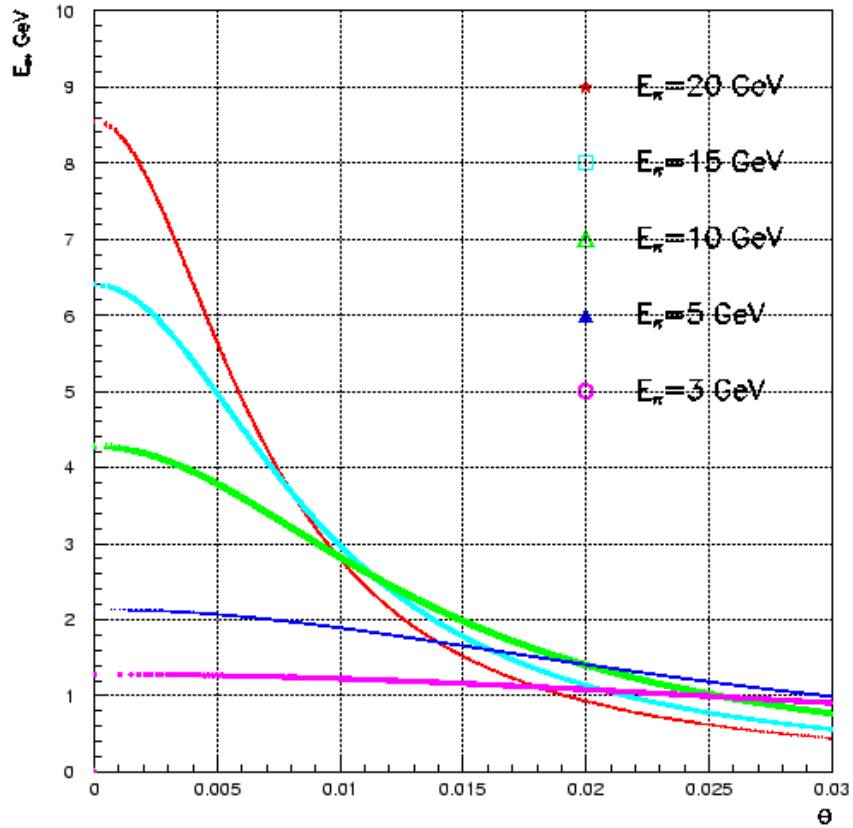


Figure 2: Variation the neutrino energy with the decay angle  $\theta_{dec}$  for neutrinos produced by  $\pi$ 's of different energies.

Figs.2 and 3 illustrate the relationship between the neutrino fluxes, energies and the decay angles for the pions in the energy ranges relevant to the NuMI beam. Neutrino flux is maximal in the forward direction,  $\theta_{dec} = 0$ , and the neutrino energy there is proportional to the energy of the parent pion,  $E_\nu = 0.43E_\pi$ . This is the reason for placing the neutrino detector 'on-axis'.

Fig.3 shows that the sharp peak of the neutrino flux in the forward direction changes into a broad maximum for pions at low energies,  $E_\pi \leq 5 \text{ GeV}$ . Low energy

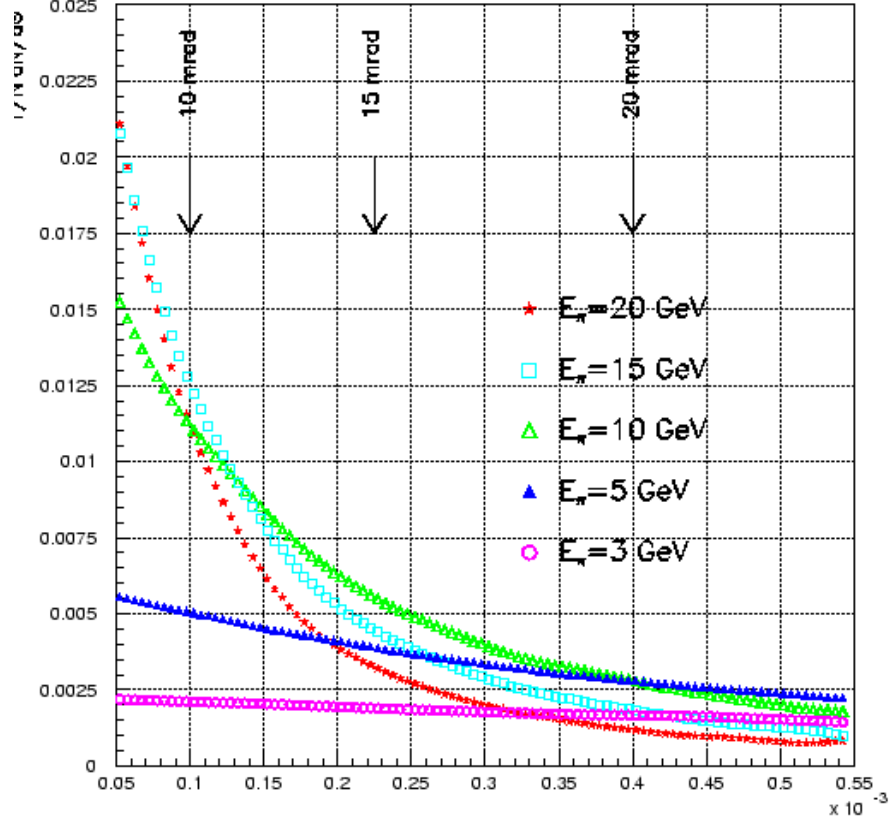


Figure 3: Variation the neutrino flux with the decay angle  $\theta_{dec}$  for neutrinos produced by  $\pi$ 's of different energies.

neutrino beam,  $E_\nu \leq 2 - 3 \text{ GeV}$ , is very broad and the detector location is not very critical for the energy and intensity of the neutrino flux. This fact makes low energy neutrino oscillation experiments relatively insensitive to the details of understanding of the underlying neutrino beam.

The same fact enables a construction of improved, with higher intensity and smaller energy spread, low energy neutrino beams. This technique, pioneered in the Brookhaven neutrino oscillation experiment proposal[3], consists of placing a neutrino detector at some angle with respect to the conventional neutrino beam.

Such a detector records approximately the same flux of low energy neutrinos, as the one positioned 'on-axis', originating from the decays of low energy pions. In addition, though, an 'off-axis' detector records an additional contribution of low energy neutrinos from the decay of higher energy pions decaying at the finite angle  $\theta_{dec}$ .

An additional attractive feature of the neutrino flux observed at the 'off-axis' detector is a kinematical suppression of high energy neutrino component. Detectors

placed at different angles with respect to the neutrino beam direction are therefore exposed to an intense narrow-band neutrino with the energy defined by the detector position.

In contrast with the traditional narrow-band neutrino beams the off-axis detectors enable a simultaneous experiments with beams at different energies/locations. At the same time the ‘off-axis’ neutrino flux is much higher than the one achievable with the traditional narrow-band beam.

## 4 Off-axis Beams at NuMI

Neutrino beam described in the previous section is directed towards a MINOS detector located in the Soudan mine. This beam, especially in its low- and medium-energy version is very broad and its energy spectrum changes significantly with the position/angle of the neutrino detector.

We consider a hypothetical situation, where the ‘on-axis’ MINOS detector is complemented by three additional detectors positioned at the transverse distance of 5, 10 and 20 km away from the central detector. For a sake of an example we examine a case of  $10 \text{ kton} \times \text{year}$  exposure.

### 4.1 Low Energy Beam Case

Fig.4 shows the expected (in ‘no oscillations’) case rates of  $\nu_\mu$  CC events in the four detectors.

As expected, the neutrino spectrum is much narrower at the ‘off-axis’ detectors than the one at the central detector, with the peak position shifting to the lower energies with the increasing distance from the beam axis. The high(er) energy tail of the spectrum is due to high momentum pions produced at relatively large angles and decaying shortly after the production target and due to kaon decays, as shown in Fig.5.

### 4.2 Medium Energy Beam Case

Expected neutrino events spectra at the ‘off-axis’ detectors in the case of the medium energy NuMI beam are shown in Fig.6.

This configuration seems to be close to the optimal running conditions. The neutrino flux in the  $3 - 4 \text{ GeV}$  region at the distance of  $5 \text{ km}$  is higher than the peak of the low energy beam ‘on-axis’, with the high energy tail greatly reduced. At the distance of  $10 \text{ km}$  the flux of the neutrinos in  $1 - 2 \text{ GeV}$  region is much higher, whereas the contribution of higher energy neutrinos is suppressed in comparison with the same detector exposed to the low energy beam in ‘on-axis’ position.



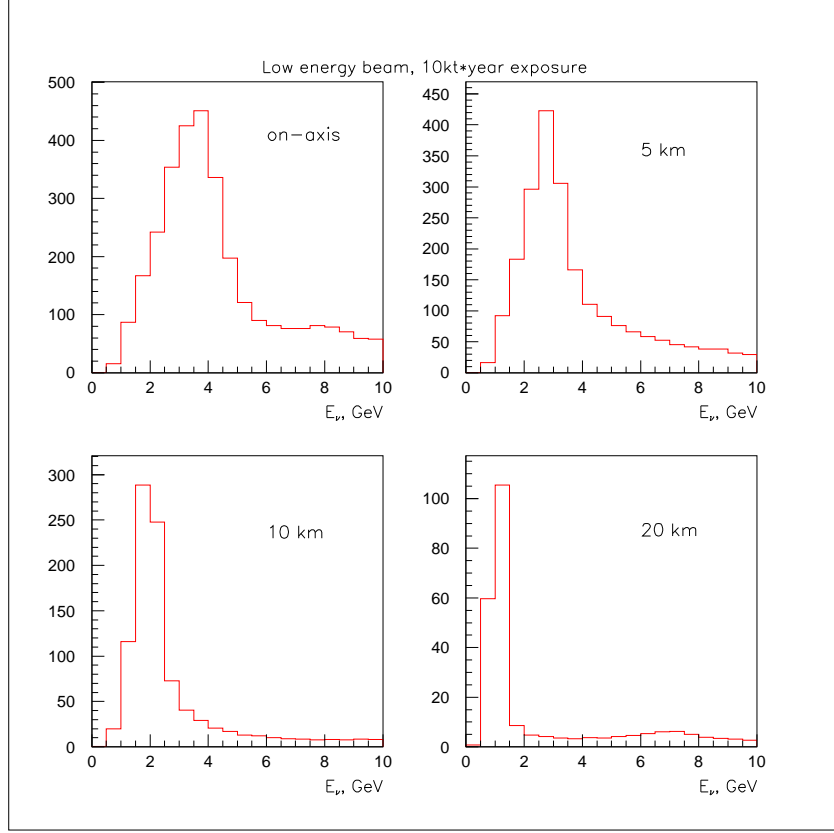


Figure 4: Low energy beam option: neutrino event spectra for 10 kton\*years exposure at the detectors on-axis and at 5,10 and 20 km distance.

### 4.3 High Energy Beam Case

High energy beam is derived from high energy pions produced in the target. At these high energies a sharp drop of the neutrino flux intensity, related primarily to the large factor  $\gamma = E_\pi/m_\pi$  in the Eq.2 leads to the effective beam intensities at the 'off-axis' detectors significantly reduced in comparison with the low and medium energy beams, as shown in Fig.7

## 5 $\nu_\mu$ Disappearance Experiment with the Off-axis Detectors

A disappearance experiment consisting of several detectors positioned at different distances from the neutrino beam axis has several attractive features:

- average energy of the neutrino beam can be selected by the position of the detectors. A suitable choice of the detectors location will enable detection of a oscillation pattern whereby the observed event rate goes down and up

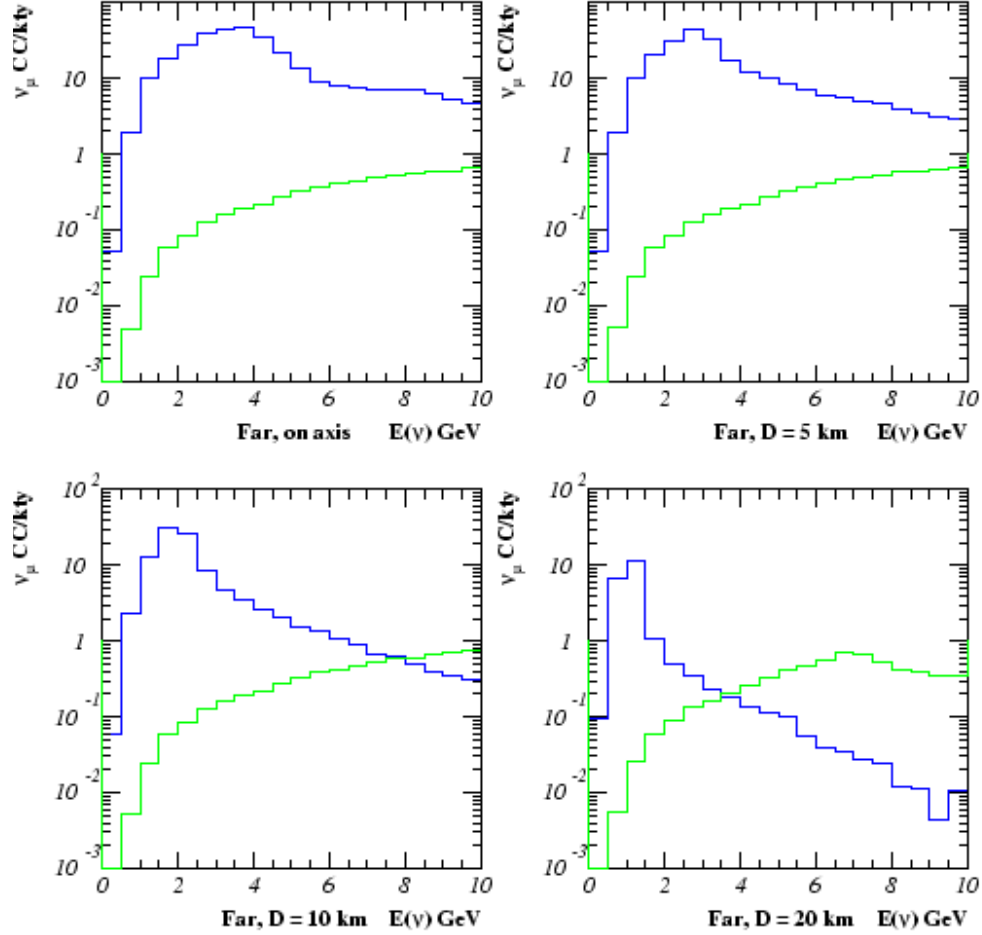


Figure 5: Contribution of pion- and kaon-produced neutrinos to the neutrino flux at the detectors on-axis and at 5,10 and 20 km distance, low energy beam.

with the increasing distance of the detector from the beam and hence with the decreasing neutrino energy, as illustrated on Fig.8.

- measurement of the disappearance of  $\nu_\mu$  CC events can be easily extended to very low energies,  $E_\nu \leq 1 \text{ GeV}$ . At these low energies the CC events will be primarily of quasi-elastic type,  $\nu_\mu + n \rightarrow \mu^- + p$  and will consist of a single penetrating muon track. In case of a wide band beam in the 'on-axis' detector such events will be contaminated by single pion events produced by the NC interactions of neutrinos at higher energies.
- a judicious choice of the detector location in conjunction with the small energy spread of the main peak of the neutrino flux enables a very precise determination of the mixing angle  $\sin^2 2\theta_{23}$ . As an example, in case of  $\Delta m_{23}^2 = 3 \times 10^{-3} \text{ GeV}$  a 10 kton detector positioned at the distance of 10 km and

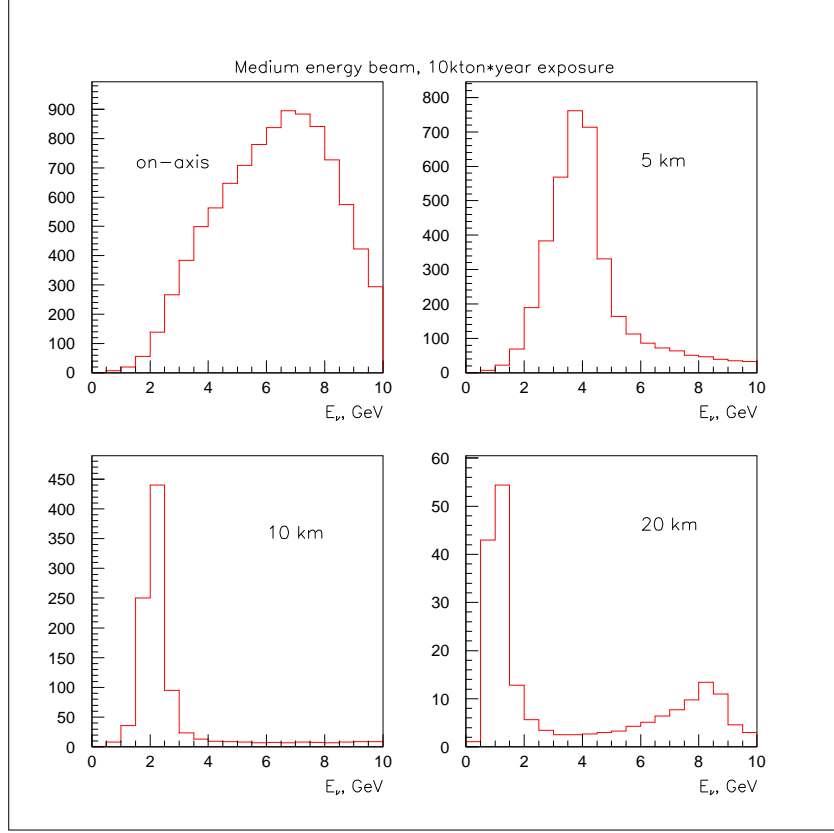


Figure 6: Medium energy beam option: neutrino event spectra for 10 kton\*years exposure at the detectors on-axis and at 5,10 and 20 km distance.

exposed to the neutrino beam produced by  $8 \times 10^{20}$  protons on target will observe 94  $\nu_\mu$  CC events instead of the expected 821 events. The number of 'missing' events provides a direct determination of the mixing angle  $\sin^2 2\theta_{23}$  with the statistical accuracy  $\Delta \sin^2 2\theta_{23} \leq 0.0014$ .

- the average energy of the neutrinos in the peak of the spectrum is determined from two-body kinematics and the detector position, independent of the detector resolution. This is a significant advantage over the wide-band neutrino beam, where the kinematical effect of the masses of the produced particles and nuclear effects introduce systematic difference between the observed (even with an ideal detector) total energy of the final state and the energy of the incoming neutrino. This effect is likely to limit the ultimate precision of the determination of  $\Delta m_{23}^2$  by the neutrino oscillation experiments, barring a breakthrough in the understanding of the intra-nuclear cascades and other nuclear effects.

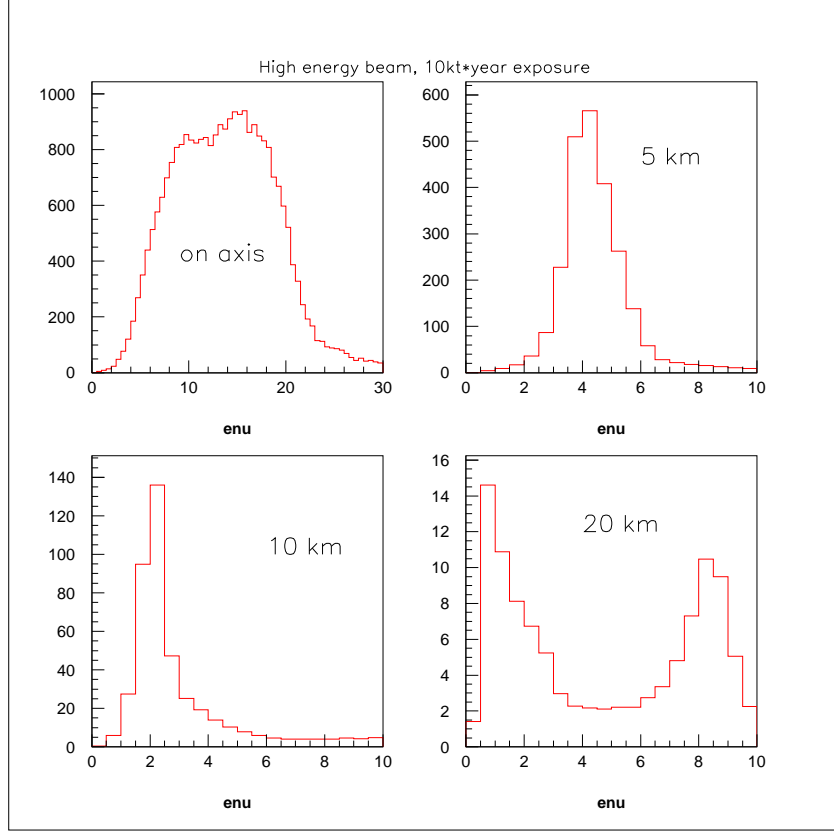


Figure 7: High energy beam option: neutrino event spectra for 10 kton\*years exposure at the detectors on-axis and at 5,10 and 20 km distance.

## 6 Systematics I: Understanding of the Beam Spectra

Well defined beam energy, determined completely by the detector position and a small energy spread make the 'off-axis' beam potentially a very powerful tool for studies of neutrino oscillations. For this purpose it is necessary, however, to be able to predict the expected neutrino beam, its spectrum and the overall normalization with adequate precision.

The far detector spectra in the 'on-axis' can be determined from the event spectra observed at the near detector. Does the experiment with 'off-axis' detector require a dedicated near experiments near the neutrino source? Such an experiment would be complicated by the extended nature of the neutrino source.

Fortunately, such an experiment is not necessary. The neutrinos observed in the near detector and in any of the far detectors are derived from the same parent beam, formed by the focusing elements. This common origin implies strong correlations between the beams observed at different locations. The correlation matrix is primarily determined by the geometry of the neutrino beam and by the details

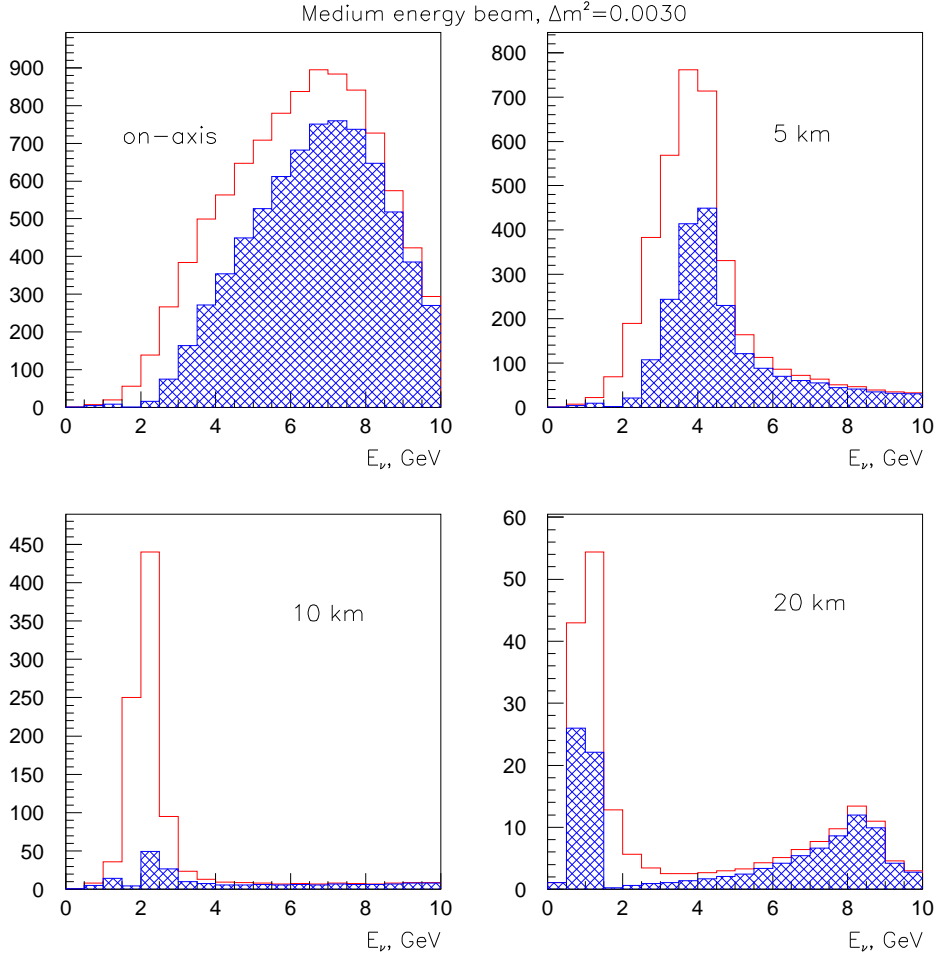


Figure 8: Expected  $\nu_\mu$  CC event rates at the on- and off-axis detectors for 10 kton\*years exposure in the medium energy beam. The histogram represents 'no-oscillation' case. The cross-hatched distribution shows the expected rate in case of oscillations with full mixing and  $\Delta m^2 = 3.0 \times 10^{-3} \text{ eV}^2$ .

of the focusing system, thus permitting an unambiguous prediction of the neutrino flux at the arbitrary position using the spectrum observed at the near detector[4]. A residual dependence on the hadron production model is very small, both for the case of the low and medium energy beams, as indicated by the Figs.9 and 10.

## 7 Systematics II: Backgrounds

The principal limitation of a sensitivity of a possible  $\nu_e$  appearance experiment will be related to the  $\nu_e$  and  $\bar{\nu}_e$  component of the beam. They are produced in  $K^+ \rightarrow \pi^0 e^+ \nu_e$  and  $\mu^+ \rightarrow e^+ \nu_e \bar{\nu}_\mu$  decays. The angular distribution of these three-body decays is somewhat different from the decays producing the main component of the  $\nu_\mu$  beam.

A relative fluxes of the  $\nu_\mu$  and  $\nu_e$  neutrinos at different detector positions are shown in Fig.11 for the low energy beam case and in Fig.12 for the medium energy

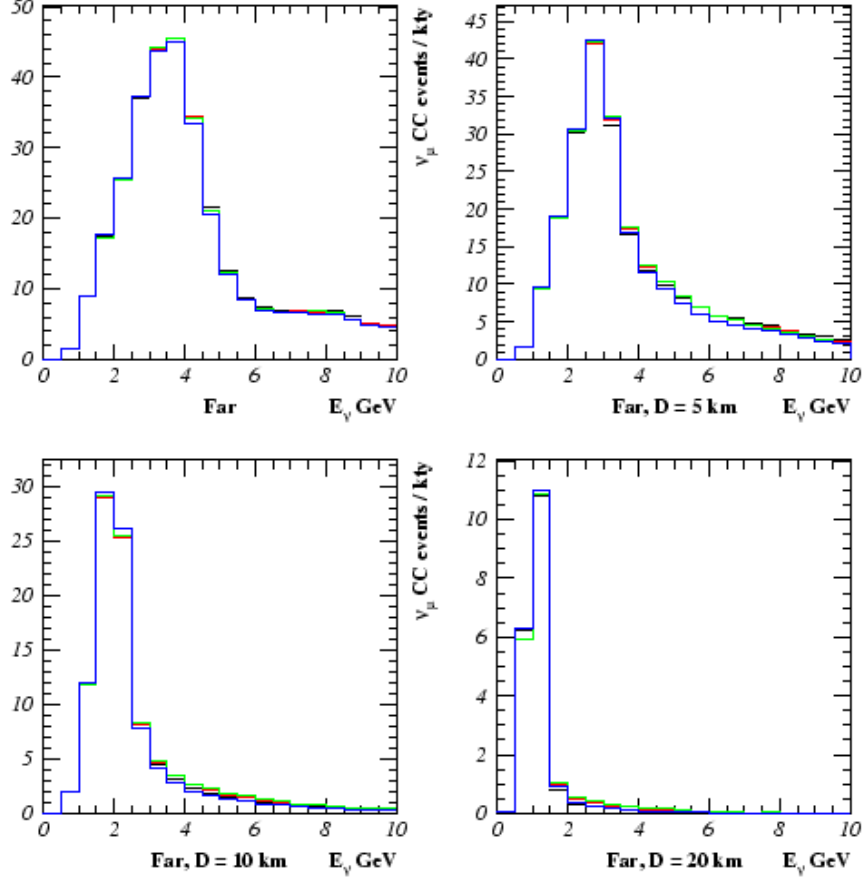


Figure 9: Dependence of the predicted neutrino spectrum on the hadron production model for the case of the low energy beam. Four overlaid histograms represent the expected spectra at different detector positions derived from the spectrum observed at the near detector using different hadron production models.

beam.

The  $\nu_e$  flux in the 'off-axis' detectors is of the order of 0.5% of the  $\nu_\mu$  flux and this background is somewhat reduced in comparison with the 'on-axis' detector.

## 8 $\nu_e$ Appearance Experiment

The primary goal of the  $\nu_e$  appearance experiments is a measurement of the  $U_{e3}$  element of the MNS neutrino mixing matrix or the mixing angle  $\sin\theta_{13}$ . The experiment is expected to detect a small number of  $\nu_e$  CC interactions among the neutrino interactions registered at the far detector. In the following we assume that the experiment is carried out at such a combination of  $L$  and  $E_\nu$  that the oscillations generated by  $\Delta m_{23}^2$  dominate and that the value of the  $\Delta m_{23}^2$  is measured precisely in the disappearance experiment. A number of the  $\nu_e$  interactions is proportional

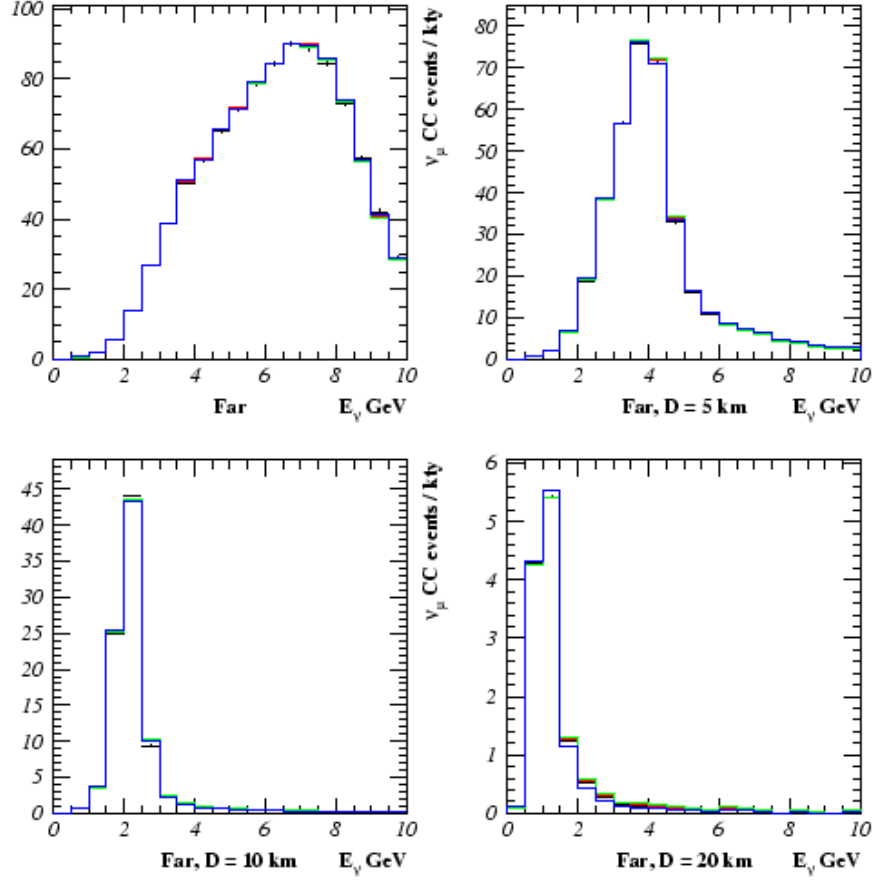


Figure 10: Dependence of the predicted neutrino spectrum on the hadron production model for the case of the medium energy beam. Four overlaid histograms represent the expected spectra at different detector positions derived from the spectrum observed at the near detector using different hadron production models.

to the neutrino mixing parameters via

$$N_{\nu_e}^{appear} = \sin^2 2\theta_{e\mu} \int dE \frac{dN_{\nu_\mu}}{dE} \sin^2 \frac{1.27 \Delta m_{23}^2 L}{E} = \sin^2 2\theta_{e\mu} N_{\nu_\mu}^{disappear} \quad (3)$$

where

$$\sin^2 2\theta_{e\mu} = \frac{1}{2} \sin^2 2\theta_{13} = 2 |U_{e3}|^2 \quad (4)$$

The  $\nu_e$  CC interactions are characterized by an absence of a long, penetrating muon track and by a presence of an electromagnetic energy cluster due to the outgoing electron. There are several sources of backgrounds yielding events with very similar characteristics:

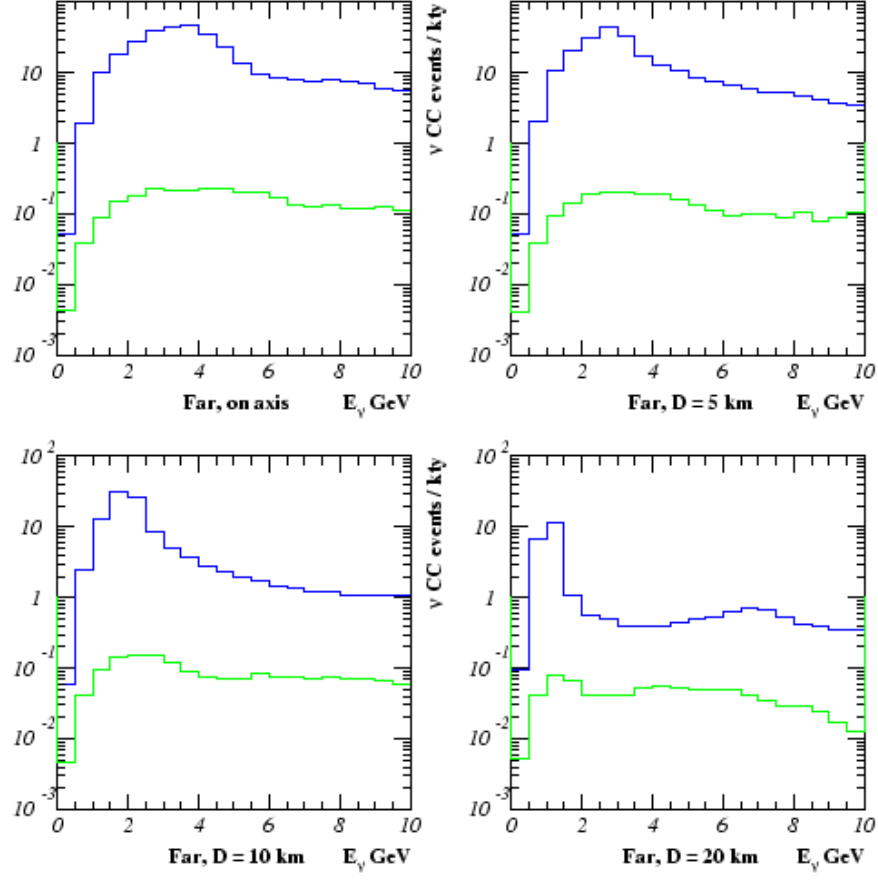


Figure 11:  $\nu_\mu$  and  $\nu_e$  induced CC event rates at the on- and off-axis detectors, low energy beam. The upper histogram represents the  $\nu_\mu$  rates, the lower one shows the  $\nu_e$  rates.

- high-y  $\nu_\mu$  CC interactions with a significant fraction of the hadronic energy produced in a form of  $\pi^0$ 's.
- NC interactions with a significant fraction of the hadronic energy produced in a form of  $\pi^0$ 's
- CC interaction of  $\nu_\tau$ 's (resulting from  $\nu_\mu \rightarrow \nu_\tau$  oscillations) with a subsequent decay  $\tau \rightarrow e$ . This background is particularly troublesome if the mixing angle  $\sin^2 2\theta_{e\mu}$  is much smaller than  $\sin^2 2\theta_{\tau\mu}$ .

An additional, irreducible, contribution to the sample of potential  $\nu_e$  CC interactions is produced by an intrinsic  $\nu_e$  component of the neutrino beam.

A sensitivity of the measurement of the mixing parameters will be limited by the statistical fluctuations of the background event sample, even if the overall normalization of the background is known. It is, therefore, very important to minimize



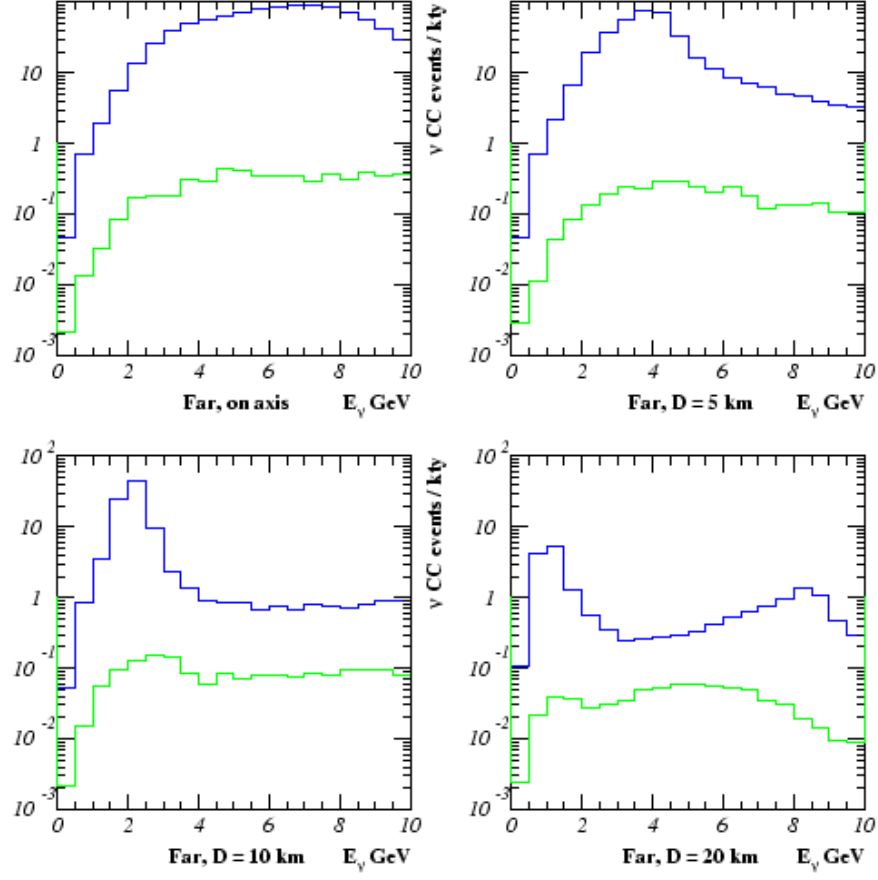


Figure 12:  $\nu_\mu$  and  $\nu_e$  induced CC event rates at the on- and off-axis detectors, medium energy beam. The upper histogram represents the  $\nu_\mu$  rates, the lower one shows the  $\nu_e$  rates.

the size of the background sample, while the sample of detected  $\nu_e$  CC interactions due to the oscillations is maximized.

The optimization procedure involves several factors:

- a judicious choice of the beam energy and spectrum. An optimal neutrino beam would have a large flux concentrated around  $E_{opt} = \frac{2.54L\Delta m_{23}^2}{\pi}$ . Such a beam would have the following effects:
  - a number of  $\nu_\mu$ 's which have 'oscillated' away,  $N_{\nu_\mu}^{disappear}$ , in Eq.3 would be maximized
  - background due to high-y  $\nu_\mu$  CC interactions would be minimized
  - background from the NC interactions would be minimized if the neutrino spectrum does not extend beyond the region where the oscillation probability is very large

- a choice of the distance of the detector from the neutrino source. To eliminate the background due to CC  $\nu_\tau$  interactions it is desirable that the optimal energy  $E_{opt}$  is below the kinematical threshold for  $\tau$  production.
- a suitable choice of the analysis cuts. Oscillations-induced  $\nu_e$  events will be concentrated in a narrow energy range around  $E_{opt}$ . A large fraction of NC events will have an observed energy much lower than the neutrino energy due to the escaping neutrino, hence a requirement that the detected energy of the event exceeds a certain fraction of the  $E_{opt}$  may significantly reduce the NC background. The intrinsic  $\nu_e$  component of the beam tends to have much harder energy spectrum (see Figs. 11 and 12), hence a requirement that the observable energy does not exceed a certain value will significantly reduce this background.

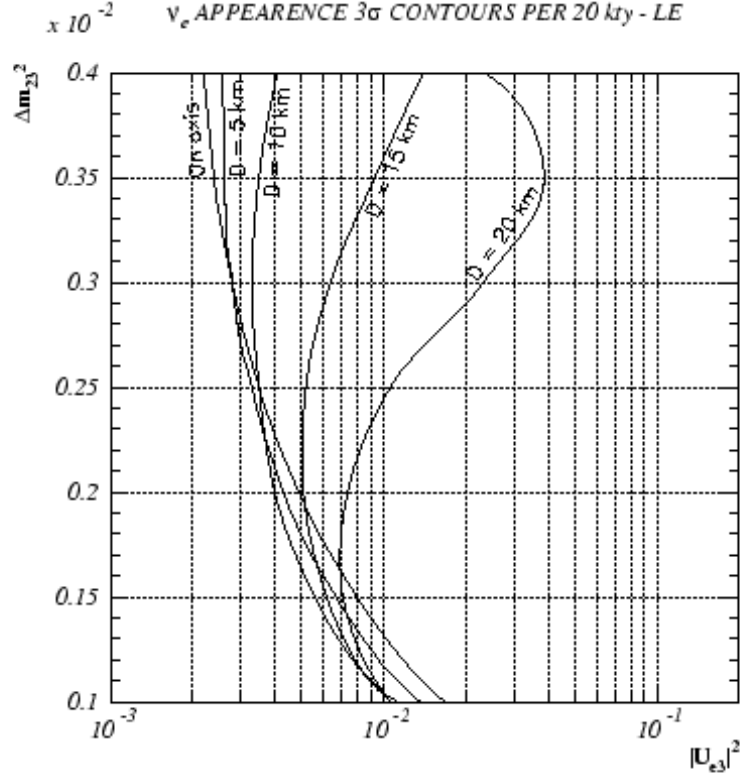


Figure 13: Sensitivity of the appearance experiments to  $|U_{e3}|_{min}^2$  for low energy beam exposure 20 kt\*years.

A potential of the  $\nu_e$  appearance experiment with the 'off-axis' detectors is shown in Figs. 13 and 14 for the case of low and medium energy beams respectively.

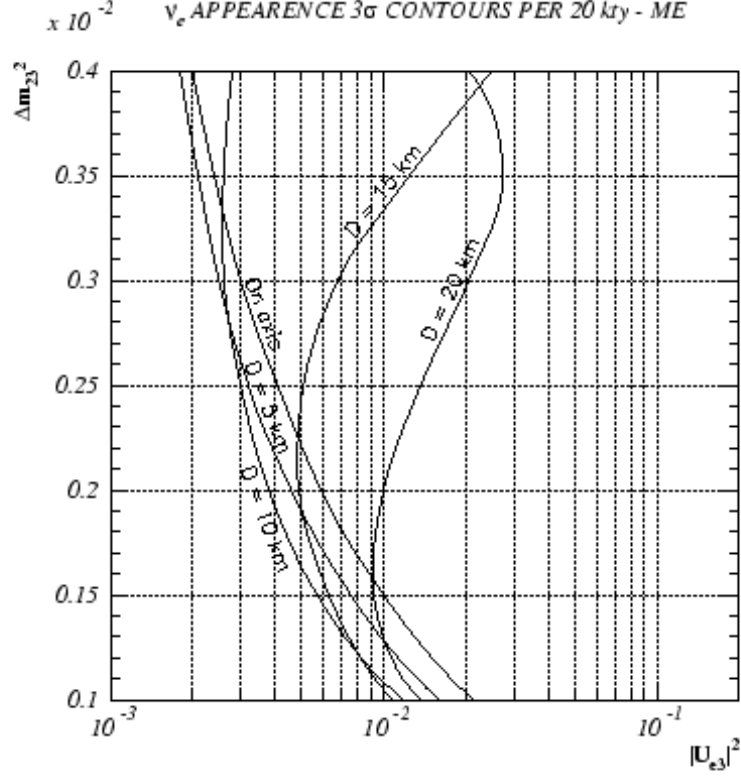


Figure 14: Sensitivity of the appearance experiments to  $|U_{e3}|_{min}^2$  for medium energy beam exposure of 20 kt\*years.

Sensitivity of the experiment to the  $|U_{e3}|^2$  is taken to be equal to the  $3\sigma$  fluctuation of the background. It is assumed that the  $\pi^0$  rejection power of the neutrino detector is sufficient to reduce the NC background to the level below the intrinsic  $\nu_e$  component of the beam. The size of the exposure is taken to correspond to 20 kton\*years at the 100% electron identification efficiency.

A detector situated at the distance of 10 km from the beam axis offers the best opportunity for the measurement of the  $|U_{e3}|^2$ . Although a potential reach of the detector located at the distance of 5 km is somewhat better for larger values of  $\Delta m_{32}^2$ , the NC background would be much larger there, thus necessitating a substantially better detector to ensure the adequate background rejection.

An example of the actual event rates for the case of medium energy beam and oscillations corresponding to  $\Delta m_{23}^2 = 0.003 \text{ eV}^2$  is shown in Table 1.

Table 1: Examples of  $\nu_e$  appearance experiments for  $\Delta m_{23}^2 = 0.003 eV^2$ .  $E_{min} - E_{max}$  denote the optimal energy range,  $\nu_\mu$  no osc./osc. are the expected numbers of  $\nu_\mu$  CC interactions without and with oscillations,  $|U_{e3}|_{min}^2$  corresponds to the value of the mixing parameters producing an effect equal to  $3\sigma$  fluctuation of the background.

Det. position, R	$E_{min} - E_{max}$ , GeV	$\nu_\mu$ no osc.	$\nu_e$ bckg.	$\nu_\mu$ osc.	$ U_{e3} _{min}^2$
0 km	1.0 - 7.5	13460	60.0	9380	0.0030
5 km	1.0 - 4.5	5420	24.0	2480	0.0025
10 km	1.5 - 2.5	1380	4.4	80	0.0024
15 km	1.0 - 1.5	320	1.0	100	0.0068
20 km	0.5 - 1.5	200	1.2	120	0.0206

## 9 Neutrino Detectors Issues

The NuMI neutrino beam is directed towards the MINOS detector located in the Soudan mine. Construction of underground facilities at the off-axis locations is not practical, therefore the design of the detectors and their locations must be optimized to enable precise measurements despite the presence of cosmic rays induced backgrounds.

Transverse distance of the detector from the beam axis determines the average energy of the neutrino beam. Thus the optimal detector position depends on the value of the  $\Delta m^2$  and on the nature of the desired measurement.

For example, if  $\Delta m^2 = 3 \times 10^{-3} eV^2$  then a detector at the transverse distance of 10 km from Soudan would be located at the maximum of the oscillation and it would be an optimal one for the measurement of the mixing angle and for the detection of  $\nu_e$  appearance. An additional detector at the distance of 20 km could be used to demonstrate the oscillation pattern.

Optimization of a possible detector location may include the variation of the distance of the putative detectors from Fermilab. Sensitivity of the neutrino oscillations appearance experiments does not depend on the experiment baseline as long as the beam energy is much higher than the one corresponding to the oscillation maximum, as  $\frac{1}{L^2}$  reduction of the flux is compensated by the increased oscillation probability  $\left(\frac{L}{E}\right)^2$ .

The situation is different when the combination of the experiment baseline  $L$  and the beam energy  $E$  corresponds to the oscillation maximum. The change of the sensitivity of the appearance experiment with the reduction of the baseline of the experiment is a combination of an increase of the neutrino flux as  $\frac{1}{L^2}$  and a reduction of the oscillation probability, if the detector is located at the same angle with the respect to the neutrino axis or a change of the neutrino flux with the increased angle if the detector is located at a larger angle to lower the neutrino energy to correspond

to the oscillation maximum at the new location. This interplay between the detector longitudinal and transverse positions is illustrated in Fig.15.

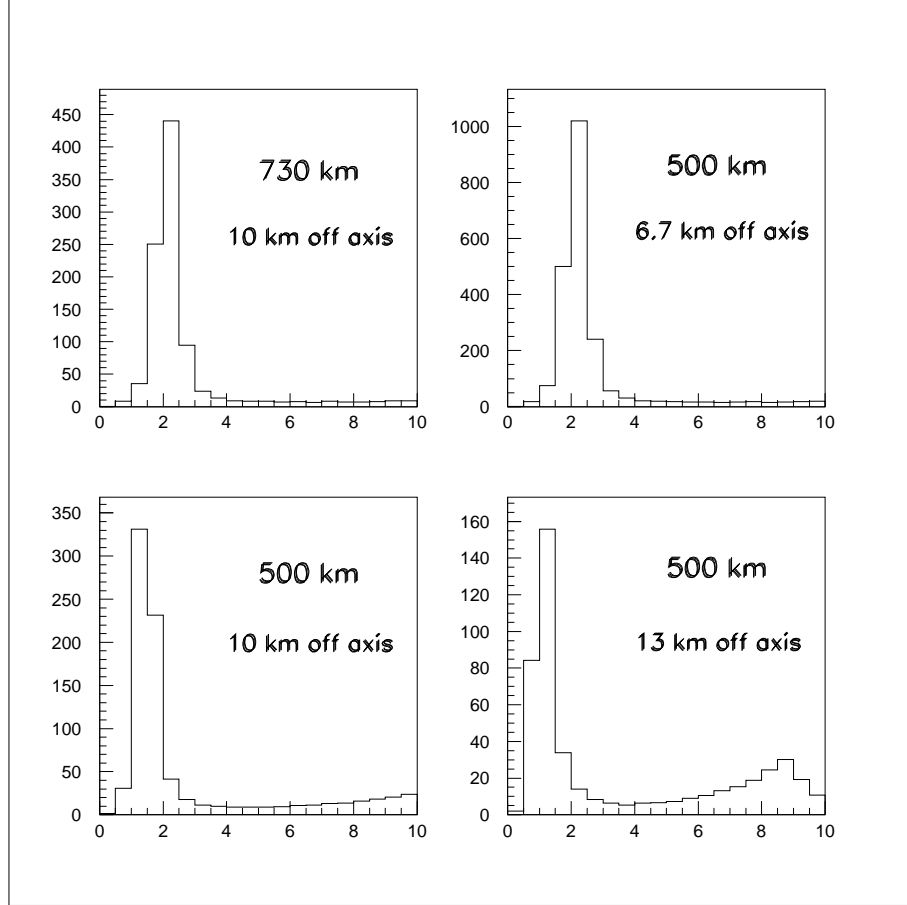


Figure 15: Rates of  $\nu_\mu$  CC event rates in the detectors located at different locations. Rates correspond to the medium energy beam,  $10 \text{ kton} \times \text{year}$  exposure

The NuMI neutrino beam has an interesting property of passing, at the distance of about  $600 \text{ km}$ , under the large body of water, the Lake Superior. It allows for an unique neutrino oscillation experiment utilizing the same detector exposed to the narrow-band neutrino beam of different energies. Such an experiment mounted on a barge floating the the Lake Superior can be moved to an arbitrary position, thus permitting the optimization of the neutrino beam as the understanding of the neutrino oscillation progresses. An experiment can be also built as submerged module(s) towed by the barges to the requested positions. Such a scenario can significantly reduce the cosmic muon background.

## 10 Acknowledgments

Numerous discussions with our colleagues from NuMI/MINOS have helped us to understand the issues presented in this paper.

This work was supported in part by grants from the Illinois Board of Higher Education, the Illinois Department of Commerce and Community Affairs, the National Science Foundation, and the U.S. Department of Energy.

## References

- [1] Y. Fukuda *et al.* Phys. Rev. Lett. 81, 1562 (1998)
- [2] The NuMI Facility Technical Design Report, Fermilab (1998)
- [3] *Long Baseline Neutrino Oscillation Experiment* BNL E889 proposal (1995)
- [4] M. Szleper and A. Para, NuMI-B-781, hep-ex/0110001